Sharply increased insect herbivory during the Paleocene–Eocene Thermal Maximum

Ellen D. Currano*†‡, Peter Wilf*, Scott L. Wing†, Conrad C. Labandeira†§, Elizabeth C. Lovelock¶, and Dana L. Royer‖

*Department of Geosciences, Pennsylvania State University, University Park, PA 16802; †Department of Paleobiology, Smithsonian Institution, Washington, DC 20560; §Department of Entomology, University of Maryland, College Park, MD 20742; ¶Department of Earth Science, University of California, Santa Barbara, CA 93106; and ‖Department of Earth and Environmental Sciences, Wesleyan University, Middletown, CT 06459

Edited by May R. Berenbaum, University of Illinois at Urbana–Champaign, Urbana, IL, and approved December 3, 2007 (received for review September 11, 2007)

The Paleocene–Eocene Thermal Maximum (PETM, 55.8 Ma), an abrupt global warming event linked to a transient increase in pCO_2, was comparable in rate and magnitude to modern anthropogenic climate change. Here we use plant fossils from the Bighorn Basin of Wyoming to document the combined effects of temperature and pCO_2 on insect herbivory. We examined 5,062 fossil leaves from five sites positioned before, during, and after the PETM (59–55.2 Ma). The amount and diversity of insect damage on angiosperm leaves, as well as the relative abundance of specialized damage, correlate with rising and falling temperature. All reach distinct maxima during the PETM, and every PETM plant species is extensively damaged and colonized by specialized herbivores. Our study suggests that increased insect herbivory is likely to be a net long-term effect of anthropogenic pCO_2 increase and warming temperatures.

Bighorn Basin | paleobotany | plant–insect interactions | rapid climate change

During the 21st century, global surface temperature is expected to increase 1.8–4.0°C as higher atmospheric concentrations of greenhouse gases (especially CO_2) are generated by human activities (1). Food webs incorporating plants and phytophagous insects account for up to 75% of modern global biodiversity (2), so their response to this anthropogenic change will have a profound effect on the biosphere. Experiments show that plants grown in elevated CO_2 tend to accumulate more carbon and have a higher carbon:nitrogen ratio; they are, therefore, nutritionally poorer (3–5), leading to an average compensatory increase in insect consumption rates (6) as nitrogen becomes limiting. Modern insect herbivory and herbivore diversity are greatest overall in the tropics (7–10), implying a broad correlation between temperature and herbivory, and Pliocene–Pleistocene fossils show rapid shifts in the geographic ranges of insects in response to climate change (11). These existing data provide limited insight into future changes, however. The complexity of plant–insect food webs makes it difficult to generalize from experiments to the response of natural ecosystems over long time scales (12). Modern and Pliocene–Pleistocene insect biogeographic patterns have not been directly linked to pCO_2 and do not document the response of plant–insect food webs to rapid increases in temperature and pCO_2. Well preserved Paleocene–Eocene fossil angiosperm leaves show insect feeding damage and, therefore, can be used to investigate the net effects of increasing temperature and pCO_2 on full plant–insect food webs over long time scales.

Beginning in the late Paleocene, global temperatures gradually warmed to the sustained Cenozoic maximum at ≈53 Ma (13). The Paleocene–Eocene Thermal Maximum (PETM) is a transient spike of high temperature and pCO_2 representing ≈100 thousand years (ky), superimposed on a longer interval of gradual warming (14, 15); it is one of the best deep-time analogues for the modern time scale of global warming. The PETM is marked by a negative carbon isotope excursion, consistent with the release of a large amount of ^{13}C-depleted carbon to the atmosphere and oceans (14). Atmospheric pCO_2 levels are estimated to have increased by a multiple of three to four (16). Additionally, global mean surface temperatures rose at least 5°C over ≈10 ky and returned to background levels after ≈100 ky (16, 17). Significant changes in terrestrial floras and faunas have been documented from the PETM. In northwestern Wyoming's Bighorn Basin, there was a transient increase in floral diversity and change in plant species composition, reflecting a northward migration of subtropical taxa (18). A major immigration of vertebrates from Europe and Asia across high-latitude land bridges also occurred (19).

In this study, the recent discovery of floras from the PETM in the Bighorn Basin of Wyoming (18, 20) allows us to evaluate the effects of atmospheric and climatic change on plant–insect associations at significantly shorter, and more ecologically and societally relevant, time scales (10^4–10^5 yr) than previously possible using the fossil record (10^6 yr; ref. 21). We conducted insect damage censuses on fossil angiosperm leaves at five sites in the Bighorn Basin positioned before, during, and after the PETM warming event [Table 1, and see supporting information (SI) Table 4 and *Methods*]. Each censused leaf was scored for the presence or absence of 50 discrete insect feeding morphotypes (ref. 26 and Fig. 1), and the results were tabulated and analyzed, allowing us to determine changes in the diversity, frequency, abundance, and host species distribution of insect damage through the studied interval.

Results and Discussion

Damage diversity is low in the earlier late Paleocene (Tiffanian 4a and 5b), sharply increases in the latest Paleocene (Clarkforkian 3), peaks during the PETM, and then returns to intermediate values during the early Eocene. Both the bulk floras (Fig. 2) and species–site pairs (Fig. 3) show a similar pattern, as do analyses of only specialized damage morphotypes (made by insects that usually eat only one or a few plant species; ref. 27) or only mine morphotypes (Figs. 2 and 3).

The PETM is also distinct in terms of the frequency of damage on its leaves: 57% of PETM leaves are damaged, compared with

Author contributions: E.D.C., P.W., S.L.W., and C.C.L. designed research; E.D.C., P.W., S.L.W., C.C.L., and E.C.L. performed research; D.L.R. contributed new analytic tools; E.D.C. analyzed data; and E.D.C., P.W., S.L.W. C.C.L., E.C.L., and D.L.R. wrote the paper.

The authors declare no conflict of interest.

This article is a PNAS Direct Submission.

Data deposition: A representative suite of host-plant voucher specimens was deposited in the Division of Paleobotany, U.S. National Museum of Natural History (USNM) (collection nos. USNM 41643, 42041, 42042, 42384, and 42395–42399).

See Commentary on page 1781.

‡To whom correspondence should be addressed at: Department of Paleobiology, Smithsonian Institution, P.O. Box 37012, MRC 121, Washington, DC 20013. E-mail: ecurrano@geosc.psu.edu.

This article contains supporting information online at www.pnas.org/cgi/content/full/0708646105/DC1.

Table 1. Sampling summary

Site collection no*	Epoch	Mammal zone	Age, Ma†	MAT, °C‡	Leaf specimens	Leaf species	Leaf species rarefied to 800 leaves§
USNM 42395–42399¶	Eocene	Wasatchian 2	55.2	16.4 ± 2.7 (25)	1,008	6	5.1 ± 0.5
USNM 42384¶	PETM (Eocene)	Wasatchian 0	55.8	20.1 ± 2.8 (20)	995	29	26.9 ± 1.3
USNM 41643¶	Paleocene	Clarkforkian 3	55.9	15.7 ± 2.4 (25)	857	16	15.9 ± 0.3
USNM 42042 (22)	Paleocene	Tiffanian 5b	57.5	10.5 ± 2.9‖	1,362	16	14.7 ± 0.9
USNM 42041 (22)	Paleocene	Tiffanian 4a	58.9	10.5 ± 2.9‖	840	7	6.9 ± 0.2

*Complete locality information is available in SI Table 4.
†Determined by using the stratigraphic framework of Secord *et al.* (23), Wing *et al*. (18), and Clyde *et al*. (24).
‡Errors are $\pm 1\sigma$.
§Errors indicate 95% confidence intervals on the rarefaction.
¶New collection.
‖New paleotemperature estimate for the late Tiffanian, using leaf margin analysis on all published Tiffanian Bighorn Basin floral lists.

15–38% for the Paleocene sites and 33% for the post-PETM site (Table 2). Individual PETM plant species have 45–94% of their leaves damaged, and all but two have >65% of leaves damaged (Fig. 4, and see SI Table 5). Tiffanian 4a species range from 28 to 48% of leaves damaged, Tiffanian 5b 10–48%, Clarkforkian 25–65%, and post-PETM 33–34%. Additionally, 7.3% of the PETM leaves have four or more types of damage, compared with 0.4–2.6% for the Paleocene sites and 1.4% for the post-PETM (Table 3).

To examine changes in damage composition and distribution through time, we performed a two-way cluster analysis (29) of the seven functional feeding groups' relative abundances on those 29 species–site pairs having at least 20 specimens per site (Fig. 4). Feeding on the individual Clarkforkian and PETM plant species (cluster 2) is distinct from that on the Tiffanian species (cluster 1) because of the rarity of the more specialized feeding groups (surface feeding, mining, galling, and piercing and sucking) in the Tiffanian. Mining and surface feeding are particularly abundant during the PETM, causing the majority of the PETM taxa to form a distinct cluster (2b) from the Clarkforkian taxa (2a). Thus, the increased diversity and frequency of damage in the PETM occurs on all plant species and is not driven by increased feeding on one particular host. All but one of the PETM plant taxa analyzed here have at least one insect mine morphotype (Fig. 1), compared with three of seven in the latest Paleocene and one each at the remaining three sites. The only abundant PETM species not mined is a small legume (dicot sp. WW001) whose leaflet area rarely exceeds 225 mm^2. Mines also occur on three of the rare PETM taxa not shown in Fig. 3.

Because the PETM plant species are not found at the other sites, we tested whether their leaves had significant structural differences that would make them more palatable to herbivores. Leaf mass per area (LMA) is linked to a variety of important plant ecological traits, including lower nutrient concentrations and thicker and tougher leaves (30, 31). Therefore, leaves with higher LMA are generally less palatable to herbivores and have less insect damage (30, 32). Fossil LMA can be estimated by using an extensive modern calibration set that demonstrates a robust scaling relationship between petiole width, squared, and leaf mass, normalized for leaf area (32). The theoretical explanation is that a wider petiole has a greater cross-sectional area that scales to support a heavier leaf. Critically, there are no site-level differences in LMA (Fig. 5; an ANOVA of LMA by sites yielded an F value of 0.15 and $P = 0.96$, 4 degrees of freedom), indicating no significant differences in leaf

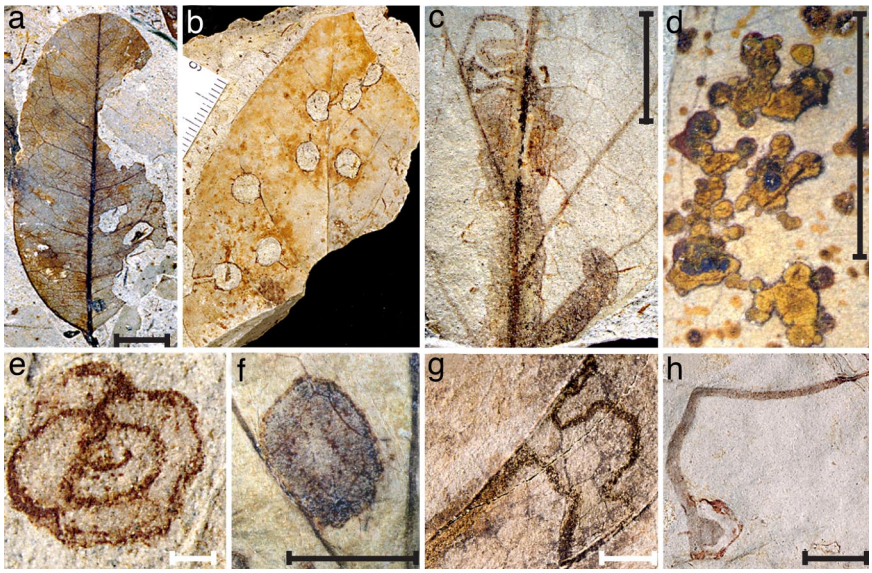

Fig. 1. Representative insect damage diversity on PETM leaves. (*a*) Dicot sp. WW007 (Fabaceae) leaf about one-third consumed by insect herbivores (USNM 530967). (*b*) Characteristic large, circular hole-feeding (DT4) found only on dicot sp. WW006 (530968). (*c*) Serpentine mine with a solid frass trail becoming massive (DT43) on an unidentifiable dicot (530969). (*d*) Polylobate to clustered galls (DT125) on dicot sp. WW007 (Fabaceae, 530970). (*e*) Blotch mine with a sinusoidal frass trail (DT37) on dicot sp. WW003 (530971). (*f*) Blotch mine with distinct coprolites and terminal chamber (DT35) on dicot sp. WW006 (530972). (*g*) Serpentine mine with a solid frass trail (DT43) on dicot sp. WW004 (530973). (*h*) Semilinear serpentine mine with terminal chamber (DT40) on dicot sp. WW005 (530974). (Scale bars: white, 1 mm; black, 5 mm.)

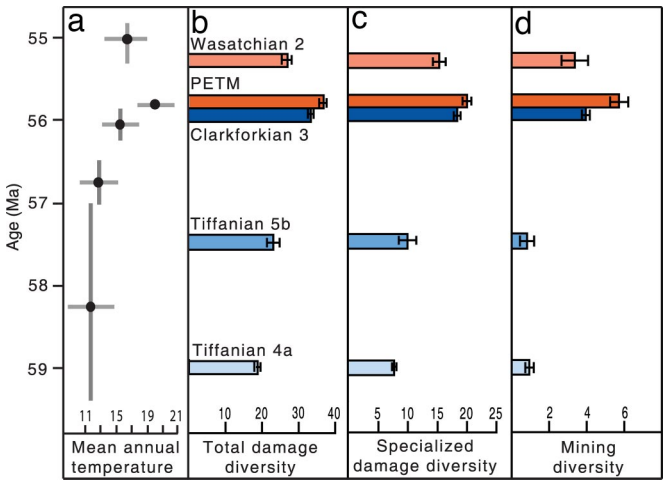

Fig. 2. Damage diversity on Paleocene–Eocene floras. (*a*) Estimates of mean annual paleotemperature through the studied interval. Additional information on these estimates is presented in Table 1. (*b*) Total damage diversity on each flora standardized to 800 leaves, with error bars representing 1 SD above and below the mean of the resamples. (*c*) Specialized damage diversity standardized as in *b*. (*d*) Diversity of mine morphotypes standardized as in *b*.

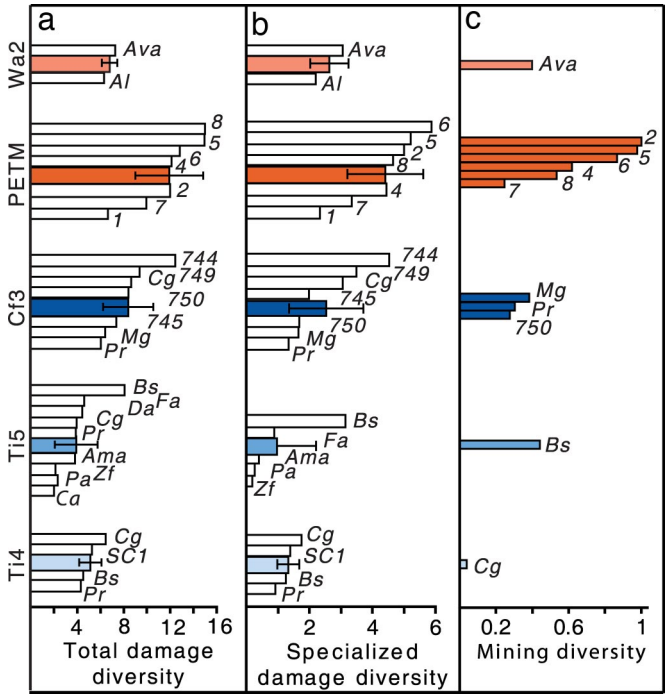

Fig. 3. Damage diversity on individual plant species. (*a*) Total damage diversity on individual plant hosts standardized to 20 leaves by resampling as in Fig. 2. Each host species with >20 specimens is represented by a white bar; colored bars represent the average damage diversity for the specified species in each flora. Plant fossils belonging to taxa that have not been formally described are referred to by morphotype number. Taxa: *Al*, *Alnus* sp. (Betulaceae); *Ama*, *''Ampelopsis'' acerifolia* (?Cercidiphyllaceae); *Ava*, *Averrhoites affinis* (?Oxalidaceae or Sapindales); *Bs*, *Browniea serrata* (Nyssaceae); *Ca*, *''Celtis'' peracuminata* (?Celtidaceae); *Cg*, *Cercidiphyllum genetrix* (Cercidiphyllaceae); *Da*, *Davidia antiqua* (Nyssaceae); *Fa*, *''Ficus'' artocarpoides* (?Platanaceae); *Mg*, *Macginitiea gracilis* (Platanaceae); *Pa*, *Persites argutus* (Lauraceae); *Pr*, *Platanus raynoldsi* (Platanaceae); *SC1*, dicot species SC1; *Zf*, *Zizyphoides flabella* (Trochodendraceae); *1*, dicot sp. WW001 (Fabaceae); *2*, dicot sp. WW002 (Fabaceae); *4*, dicot sp. WW004; *5*, dicot sp. WW005; *6*, dicot sp. WW006; *7*, dicot sp. WW007 (Fabaceae); *8*, dicot sp. WW008 (Salicaceae); *744*, dicot sp. FU744 (Betulaceae); *745*, dicot sp. FU745 (?Sapindaceae); *749*, dicot sp. FU749; *750*, dicot species FU750 (Fabaceae). Site abbreviations: Ti4, Tiffanian 4a; Ti5, Tiffanian 5b; Cf3, Clarkforkian 3; Wa2, Wasatchian 2. (*b*) Specialized damage diversity, presented as in *a*. (*c*) Diversity of mine morphotypes. Each species is represented by a bar color-coded according to flora, and taxon abbreviations are as in *a*.

properties between the PETM species and the species found at the other sites. Nearly all plant species from all five sites have low estimated LMA that would be consistent with high palatability (SI Table 5 and Fig. 5).

Increases in insect damage diversity in the Bighorn Basin in the late Paleocene and early Eocene correlate positively with increasing temperature. The first significant change in insect damage composition and diversity occurs between the late Tiffanian and late Clarkforkian, a time when both plant diversity (Table 1) and many of the dominant floral elements remain constant despite rising temperatures (33). A contemporary increase in herbivory from the Tiffanian to Clarkforkian, also without significant plant turnover, has been observed in southwestern Wyoming (22). The late Paleocene and PETM increases in diversity of herbivory do not reflect a long-term radiation of insect herbivores because damage diversity decreases after the PETM, as temperature again declines. Therefore, increases in damage diversity, particularly of specialized feeding groups, may represent an influx of thermophilic herbivores to the midlatitude regions, rather than an *in situ* diversification and accommodation. Because the geographic ranges of plant species shifted significantly during the PETM, some insects may simply have followed their host plants to the Bighorn Basin. By the middle of the PETM, every plant species represented by at least 20 censused leaves had been colonized by specialized herbivores.

We attribute the peak in insect feeding frequency during the PETM to the estimated tripling of atmospheric pCO_2 and the associated abrupt temperature rise. The major increase in plant consumption is consistent with predicted effects of elevated pCO_2 on foliar nitrogen concentration. Additionally, our damage diversity and frequency data indicate that both insect diversity and population density probably increased with temperature, although populations may have been limited by the decrease in food quality. The dramatic rise in diversity and frequency of herbivore attack on all abundant plant species during the PETM suggests that anthropogenic influence on atmosphere and climate will eventually have similar consequences.

Table 2. Percentage of leaves damaged in each flora

	Flora				
Damage	Ti4	Ti5	Cf3	PETM	Wa2
No damage	65.5 ± 1.6	85.1 ± 1.0	62.2 ± 1.7	47.2 ± 1.6	67.0 ± 1.5
Damage	34.5 ± 1.6	14.9 ± 1.0	37.8 ± 1.7	57.3 ± 1.6	33.0 ± 1.5
Specialized damage	13.2 ± 1.2	0.8 ± 0.2	13.4 ± 1.2	21.6 ± 1.3	17.1 ± 1.2
Mines	0.1 ± 0.1	0.1 ± 0.1	1.1 ± 0.4	1.8 ± 0.4	0.7 ± 0.3

Because leaves can either have damage or not have damage, sampling error can be quantified by using the equation for the standard deviation of binomially distributed outcomes (28). Errors are $\pm 1\sigma$.

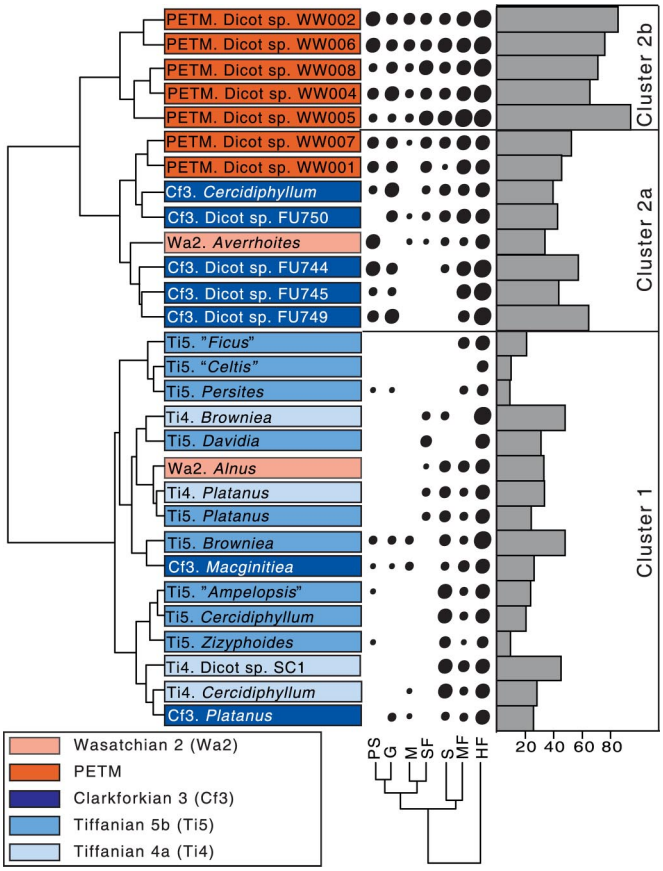

Fig. 4. Two-way cluster analysis (29) of insect damage on each plant host with >20 leaf specimens. Abbreviations for plant taxa as in Fig. 2. Functional feeding groups: HF, hole feeding; MF, margin feeding; S, skeletonization; SF, surface feeding; M, mining; G, galling; PS, piercing and sucking. The dots are scaled according to the relative abundance of each functional feeding group on each plant host. The bar graph shows the percentage of leaves of each taxon that have feeding damage.

Methods

Data Collection. We analyzed 5,062 fossil leaves from five sites with well resolved ages (18, 23) that span 3.7 My of the late Paleocene (Tiffanian–Clarkforkian) and early Eocene (Wasatchian) warming and subsequent cooling (Table 1, and see SI Table 4 and *SI Methods*). All five sites represent deposition in similar alluvial environments, and the leaf assemblages are parautochthonous. Fossil leaves and their insect damage were quantitatively censused from single stratigraphic horizons at each site. The three Paleocene sites have low plant diversity (Table 1), and the taxa are those typically found throughout the western interior of North America during the late Paleocene (34); the youngest Paleocene site is only ≈100 ky older than the PETM. The new site from the middle of the PETM carbon isotope excursion contains a diverse and unique flora for the Bighorn Basin (20). An early Eocene site postdating the PETM carbon isotope excursion by ≈0.6 My represents a return to pre-PETM temperatures, well before temperatures reached their Cenozoic maximum at ≈53 Ma.

Every morphologically identifiable, non-monocot angiosperm leaf (or leaflet for compound leaves) with more than half of the blade intact was scored for the presence/absence of 50 insect feeding morphotypes (26). A representative suite of voucher specimens is deposited in the Division of Paleobotany, U.S. National Museum of Natural History (USNM), under the collection numbers in Table 1. The complete census data are available in SI Dataset 1. These damage types (DTs) can be classified into seven functional feeding groups: hole feeding (HF), margin feeding (MF), skeletonization (S), surface feeding (SF), galling (G), mining (M), and piercing-and-sucking (PS), as described elsewhere (26, 35). The DTs can also be classified (26) as most likely to be specialized (made by insects that typically consume only one or a few closely related plant species) or generalized (typically made by polyphagous insects, e.g., most holes). Specialized feeding is delineated on evidence from extant analog feeders, morphologically stereotyped damage patterns, and restricted occurrences confined to particular host-plant species or tissue types in either fossil or extant host taxa (35).

Table 3. Percentage of leaves in each flora with a given number of damage types

No of damage types	Flora				
	Ti4	Ti5	Cf3	PETM	Wa2
1	24.4	10.5	19.7	27.9	16.5
2	8.3	3.3	8.5	14	10.3
3	1.3	0.7	7	8	4.9
4	0.5	0.3	1.8	3.6	1.1
5		0.1	0.7	1.8	0.3
6			0.1	0.4	
7				1.1	
8				0.3	
9					
10				0.1	

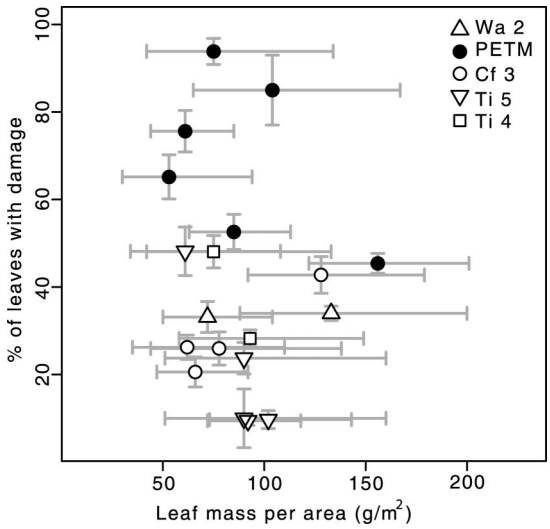

Fig. 5. Estimated LMA using the method of Royer *et al.* (32) and damage frequency for individual plant species from each site. LMA values are species means, and error bars represent the ±95% prediction interval. Errors in herbivory represent $\pm 1\sigma$, based on a binomial sampling distribution. Site abbreviations as in Fig. 2.

Quantitative Analyses of Insect Damage. All analyses were done using R version 2.2.0 (www.r-project.org). The sample size for each flora was standardized by selecting a random subset of 800 leaves without replacement and calculating the damage diversity for the subsample. This process was repeated 5,000 times, and the results were averaged to obtain the standardized damage diversity for the flora. The SD for the resamples was calculated to provide error bars. The same procedure was used to standardize insect diversity to 20 leaves on each of the 29 species–site pairs with at least 20 specimens.

The two-way cluster analysis was performed by using a data matrix in which each cell is the proportion of leaves of species *i* at site *j* that had damage belonging to functional feeding group *k*. Data were square-root transformed. R's ''agnes'' function was then used to perform agglomerative hierarchical clustering analyses (29), using Euclidean distances between samples and Ward's method of clustering. The agglomerative coefficient, a dimensionless number between 0 and 1 that describes the strength of the clustering structure, is 0.89 for clustering of plant species and 0.65 for the clustering of functional feeding groups. The raw, proportional data were log-transformed and placed into bins of 0 to −0.5, −0.5 to −1, −1 to −1.5, −1.5 to −2, and less than −2; these bins were assigned successively smaller dot sizes in Fig. 3.

Estimation of LMA. Every fossil leaf that clearly showed the attachment of the petiole to the leaf blade and had a reconstructable leaf area was used in the analysis. Eighty-five leaves, representing 19 species–site pairs, fit these criteria. Each fossil was digitally photographed and extracted from the matrix by using Photoshop (Adobe). Measurements were made using Image J (http://rsb.info.nih.gov/ij), and LMA (see SI Table 5 and Fig. 5) was calculated using the protocol of Royer *et al.* (32).

ACKNOWLEDGMENTS. We thank P. Anderson, B. Cariglino, D. Danehy, W. Gallagher, K. Galligan, F. Marsh, T. Menotti, M. Nowak, S. Lyles, F. Smith, and K. Werth for field assistance; J. Bonelli, G. Hunt, M. Patzkowsky, J. Sessa, and M. Westoby for discussion; and two anonymous reviewers for constructive comments. This work was supported by the Evolving Earth Foundation; the Geological Society of America; National Science Foundation (NSF) Grants EAR-0120727 and EAR-0236489; the NSF Graduate Research Fellowship Program; the Paleontological Society; the David and Lucille Packard Foundation; Pennsylvania State University; Petroleum Research Fund Grants 35229-G2 and 40546-AC8; the Roland Brown Fund; and the University of Pennsylvania. This is contribution no. 170 of the Evolution of Terrestrial Ecosystems Consortium at the Smithsonian National Museum of Natural History.

1. Alley R, Berntsen T, Bindoff NL, Chen Z, Chidthaisong A, Friedlingstein P, Gregory J, Hegel G, Heimann M, Hewitson B, *et al.* (2007) *Climate Change 2007: The Physical Science Basis, Summary for Policymakers* (Intergovernmental Panel on Climate Change Secretariat, Geneva).
2. Price PW (2002) *Ecol Res* 17:241–247.
3. Bazzaz FA (1990) *Annu Rev Ecol Syst* 21:167–196.
4. Lincoln DE, Fajer ED, Johnson RH (1993) *Trends Ecol Evol* 8:64–68.
5. Whittaker JB (2001) *J Ecol* 89:507–518.
6. Watt AD, Whittaker JB, Docherty M, Brooks G, Lindsay E, Salt DT (1995) in *Insects in a Changing Environment*, eds Harrington R, Stork N (Academic, San Diego), pp 198–217.
7. Coley PD, Aide TM (1991) in *Plant–Animal Interactions: Evolutionary Ecology in Tropical and Temperate Regions*, eds Price PW, Lewinsohn TM, Fernandes GW, Benson WW (Wiley, New York), pp 25–49.
8. Moran VC, Southwood TRE (1982) *J Anim Ecol* 51:289–306.
9. Price PW (1991) in *Plant–Animal Interactions: Evolutionary Ecology in Tropical and Temperate Regions*, eds Price PW, Lewinsohn TM, Fernandes GW, Benson WW (Wiley, New York), pp 51–69.
10. Stork NE (1987) *Ecol Entomol* 12:69–80.
11. Coope G (1995) in *Insects in a Changing Environment*, eds Harrington R, Stork N (Academic, San Diego), pp 29–48.
12. Zvereva EL, Kozlov MV (2006) *Global Change Biol* 12:27–41.
13. Zachos J, Pagani M, Sloan L, Thomas E, Billups K (2001) *Science* 292:686–693.
14. Zachos JC, Rohl U, Schellenberg SA, Sluijs A, Hodell DA, Kelly DC, Thomas E, Nicolo M, Raffi I, Lourens LJ, *et al.* (2005) *Science* 308:1611–1615.
15. Gradstein FM, Ogg JG, Smith AG, eds (2004) *A Geologic Time Scale 2004* (Cambridge Univ Press, Cambridge, UK).
16. Zachos JC, Wara MW, Bohaty S, Delaney ML, Petrizzo MR, Brill A, Bralower TJ, Premoli-Silva I (2003) *Science* 302:1551–1554.
17. Rohl U, Bralower TJ, Norris RD, Wefer G (2000) *Geology* 28:927–930.
18. Wing SL, Harrington GJ, Smith FA, Bloch JI, Boyer DM, Freeman KH (2005) *Science* 310:993–996.
19. Gingerich PD (2006) *Trends Ecol Evol* 21:246–253.
20. Wing SL, Lovelock EC, Currano ED (2006) in *Climate and Biota of the Early Paleogene* (Bilbao, Spain), Vol of Abstracts.
21. Wilf P, Labandeira CC (1999) *Science* 284:2153–2156.
22. Wilf P, Labandeira CC, Johnson KR, Ellis B (2006) *Science* 313:1112–1115.
23. Secord R, Gingerich PD, Smith ME, Clyde WC, Wilf P, Singer BS (2006) *Am J Sci* 306:211–245.
24. Clyde WC, Hamzi W, Finarelli JA, Wing SL, Schankler D, Chew A (2007) *Geol Soc Am Bull* 119:848–859.
25. Wing SL, Bao H, Koch PL (2000) in *Warm Climates in Earth History*, eds Huber BT, MacLeod KG, Wing SL (Oxford Univ Press, Cambridge, UK), pp 197–237.
26. Labandeira CC, Wilf P, Johnson KR, Marsh F (2007) *Guide to Insect (and Other) Damage Types on Compressed Plant Fossils*. Version 3.0. Available at http://paleobiology.si.edu/insects/index.html.
27. Labandeira CC, Johnson KR, Wilf P (2002) *Proc Natl Acad Sci USA* 99:2061–2066.
28. Wilf P (1997) *Paleobiology* 23:373–390.
29. Kaufman L, Rousseeuw PJ (1990) *Finding Groups in Data: An Introduction to Cluster Analysis* (Wiley, New York).
30. Coley PD, Barone JA (1996) *Annu Rev Ecol Syst* 27:305–335.
31. Wright IJ, Reich PB, Westoby M, Ackerly DD, Baruch Z, Bongers F, Cavender-Bares J, Chapin T, Cornelissen JHC, Diemer M, *et al.* (2004) *Nature* 428:821–827.
32. Royer DL, Sack L, Wilf P, Lusk CH, Jordan GJ, Niinemets Ü, Wright IJ, Westoby M, Cariglino B, Coley PD, *et al.* (2007) *Paleobiology* 33:574–589.
33. Wing SL, Harrington GJ (2001) *Paleobiology* 27:539–563.
34. Brown RW (1962) *Paleocene Flora of the Rocky Mountains and Great Plains* (US Geol Surv, Reston, VA), Prof Pap 375.
35. Labandeira CC (2002) in *Plant–Animal Interactions: An Evolutionary Approach*, eds Herrera CA, Pellmyr O (Blackwell Science, Oxford), pp 26–74.